

# Impact of Intraoperative 3-Tesla MRI on Endonasal Endoscopic Pituitary Adenoma Resection and a Proposed New Scoring System for Predicting the Utility of Intraoperative MRI

Masahiro TANJI,<sup>1</sup> Hiroharu KATAOKA,<sup>1</sup> Masahiro KIKUCHI,<sup>2</sup>  
Tatsunori SAKAMOTO,<sup>2</sup> Fumihiko KUWATA,<sup>2</sup> Mami MATSUNAGA,<sup>2</sup>  
Takayuki NAKAGAWA,<sup>2</sup> Yohei MINEHARU,<sup>1</sup> Yoshiki ARAKAWA,<sup>1</sup>  
Kazumichi YOSHIDA,<sup>1</sup> and Susumu MIYAMOTO<sup>1</sup>

<sup>1</sup>Department of Neurosurgery, Kyoto University Graduate School of Medicine, Kyoto, Kyoto, Japan

<sup>2</sup>Department of Otolaryngology, Head and Neck surgery, Kyoto University Graduate School of Medicine, Kyoto, Kyoto, Japan

## Abstract

The aim of this study was to evaluate the impact of 3-Tesla intraoperative high-field magnetic resonance imaging (3T-iMRI) for pituitary adenoma resection, and to propose a new scoring system for predicting the utility of 3T-iMRI. This retrospective study evaluated 82 patients with pituitary adenoma who underwent purely endoscopic endonasal resection with 3T-iMRI between 2015 and 2019. 3T-iMRI revealed unexpected residual tumor in 39 cases (47.6%), which led to further resection and contributed to upgrading of the resection level in 28 cases (34.1%), which led to gross total resection rates (GTRs) of 67.1% and near total resection of 15.9%. To construct a new scoring system, patients were divided into a discovery cohort (56 patients) and a validation cohort (26 patients). Three variables for the scoring system were selected according to a univariate analysis of the discovery cohort: the size of the tumor (>20 mm: 1 point), the presence of suprasellar tumor lobulation (1 point) and the history of previous operations (1 point). The risk of additional resection after iMRI was well stratified by this scoring system (range 0–3;  $p = 0.0037$  for trend). Robustness of the system was confirmed in the validation cohort (0 points, 0%; 1 point, 30.8%; 2 points, 70.0%; 3 points, 100%;  $p = 0.0116$  for trend). These results indicate that 3T-iMRI optimized the extent of resection, even with the use of an endoscope, and that the proposed scoring system is useful for predicting whether 3T-iMRI is likely to be of value for a particular patient.

Keywords: intraoperative MRI, pituitary surgery, transsphenoidal surgery, pituitary score, Knosp grade

## Introduction

The introduction of the endoscope into transsphenoidal pituitary surgery and its provision of a panoramic view has expanded the scope of the accessible area compared with traditional operating microscopes.<sup>1,2)</sup> Intraoperative magnetic resonance imaging (iMRI) is also reported to be useful for maximal safe resection

of pituitary adenoma.<sup>3,4)</sup> However, few studies have analyzed the added value of iMRI in purely endoscopic pituitary adenoma surgery,<sup>3–9)</sup> particularly the use of high-field iMRI.<sup>6,10)</sup> Furthermore, the possible indications for high-field iMRI have not been fully elucidated.<sup>11,12)</sup> The high cost and increased operative time<sup>13)</sup> associated with high-field iMRI must be balanced against the improved outcomes obtained, and identifying patients for whom iMRI is of particular value is critical when considering whether to install and utilize iMRI. In the current study, we investigated the clinical value of 3-Tesla (3T)-iMRI for detecting residual tumor in endoscopic endonasal pituitary adenoma resection, and evaluated its impact

Received February 24, 2020; Accepted July 6, 2020

Copyright© 2020 by The Japan Neurosurgical Society This work is licensed under a Creative Commons Attribution-NonCommercial-NoDerivatives International License.

on resection extent. Based on our experience, we propose a new four-tier scoring system to predict the utility of 3T-iMRI for individual patients.

## Materials and Methods

### Patient demographics

Patients who underwent fully endonasal endoscopic transsphenoidal surgery for tumor resection with 3T-iMRI between July 2015 and Oct 2019 at the Department of Neurosurgery, Kyoto University Hospital, were retrospectively reviewed. The inclusion criteria included the availability of preoperative and intraoperative imaging. Patients undergoing transcranial or combined procedures were excluded. 3T-iMRI was conducted routinely, unless it was medically contraindicated. Emergency cases for which 3T-iMRI was unavailable were also excluded. The patients were further divided randomly into a discovery cohort (two-thirds of patients) and a validation cohort (one-third of patients) using a random number generator. This study was approved by the Ethics Committee of Kyoto University Graduate School of Medicine (IRB-R2088-1) and qualified for a waiver for the requirement for individual patient consent.

### Neuroimaging and Data acquisition

All patients included in the study underwent preoperative, intraoperative, and 2–12 months postoperative MRI imaging. The preoperative and intraoperative MRI acquisition included whole-brain diffusion-weighted, axial T2-weighted, and post-contrast 3D T1-weighted sequences. Post-contrast 3D T1-weighted images were included for updating the navigation of the electromagnetic field navigation system.

Patients were also classified into two groups: an “intention for complete resection” group, in which the surgical goal was gross total resection (GTR); and an “intention for partial resection” group, in which the surgical goal was partial or subtotal resection because GTR was deemed not possible because of preoperative adenoma extension. The tumor remnants detected by iMRI were classified according to their location: intrasellar, cavernous sinus, suprasellar, or subdural.

The suprasellar lobulation ratio was defined as the ratio between the maximal suprasellar horizontal diameter and the diaphragm on coronal preoperative contrast-enhanced T1-weighted imaging with the ratio being defined as 1 when there was no suprasellar extension.

### Endoscopic endonasal surgery and intraoperative imaging

All surgical procedures were performed by the same surgical team comprising a single neurosurgeon

(MT) and a team of otorhinolaryngologists (TS, FK, MM, MK, and TN). The standard surgical protocol was as follows. A standard endonasal endoscopic approach using the common bi-nostril three or four-hand technique was performed. The patients were placed in a supine position without fixing the head and were registered for the electromagnetic field-based image-guided navigation system (Fusion ENT, Medtronic, Minneapolis, MN, USA). A 2D rigid endoscope (Karl Storz, Tuttlingen, Germany) was mostly used for visualization. After the neurosurgeon declared that the resection was complete or felt that further resection was unsafe, the surgery was interrupted and 3T-iMRI (Magnetom Verio, SIEMENS, Munich, Germany) was performed. The MRI sequences acquired included 3D T1-weighted images (1- to 3-mm slice thickness) obtained before and approximately 5 minutes after injection of a gadolinium contrast agent. When 3T-iMRI confirmed GTR or achievement of the surgical goal, the surgery was completed. All suspected cerebrospinal fluid (CSF) leaks were repaired using a modified graded repair protocol.<sup>14)</sup> The surgical field was inspected for any CSF leaks using the Valsalva maneuver. When there was concern about resectable residual tumor detected by iMRI, the navigation data were updated and further inspection and resection were performed. When necessary, a second iMRI was performed after second-look surgery.

### Proposed scoring system (Kyoto Pituitary Score)

The proposed new scoring system is a four-tier grading score based on three variables: the size of the tumor ( $>20$  mm or  $\leq 20$  mm), the presence of suprasellar tumor lobulation (suprasellar lobulation ratio  $>1.1$  or  $\leq 1.1$ ), and the history of past operations. Additional tumor resection after iMRI was compared between the grades to evaluate the benefit of iMRI both in the discovery cohort and the validation cohort.

### Data analysis

Patient demographic and outcome data are presented as mean (standard deviation), count, or percentage. The degree of resection was rated as follows: total, 100%; near total, 95% or greater; subtotal, 80%–95%; and partial, when the resection was less than 80%. The degree of resection was assessed on postoperative MRI 2–12 months after surgery. Receiver operating characteristic (ROC) curve analysis was performed to determine the cutoff value to stratify the risk of additional resection after iMRI. Univariate and multivariate logistic regression analyses were performed. The variables included preoperative maximum tumor diameter, Knosp grade, the number

of prior surgeries, suprasellar lobulation ratio, and intention for GTR or STR. Comparisons between the groups were made using Fisher's exact test. Statistical analyses were performed using Graphpad Prism ver 6.0 (GraphPad Software, San Diego, CA, USA) and R statistical software (<https://www.r-project.org>).

## Results

### Demographics

During the study period, 175 endoscopic endonasal operations were performed. Among these, data for 82 operations for pituitary adenoma with intraoperative 3T-MRI were analyzed. The baseline clinical characteristics of the patients are summarized in Table 1. There were 51 female and 31 male patients ranging in age from 19 to 82 years (mean: 55.8 years). The pathological diagnosis was non-functioning pituitary adenoma in 56 patients and functioning pituitary adenoma in 20 patients (Cushing disease: 5 patients; GHoma: 14 patients; PRLoma: 3 patients; TSHoma: 1 patient). In all, 25 patients (31.3%) had undergone prior surgical treatment for their lesions, and seven of them had undergone multiple surgical treatments.

Among the 82 patients with pituitary adenoma, five had microadenoma (diameter <1 cm) and 77 had macroadenoma (diameter >1 cm). The average preoperative maximal tumor diameter was 23.8 mm (range: 6–43.0 mm). The Knosp grade was grade 0 in one patient, grade 1 in 15 patients, grade 2 in 23 patients, grade 3 in 28 patients, and grade 4 in 15 patients. Suprasellar extension was present in 63 cases (76.8%).

### Impact of iMRI on the extent of resection for pituitary adenoma

The 3T-iMRI revealed unexpected residual tumor in 39 (47.6%) of the 82 patients, including two unexpected hematomas, and further resection led to GTR in 55 patients (67.1%), near total resection in 13 patients (15.9%), subtotal resection in 11 patients (13.4%), and partial resection in three patients (3.7%; Fig. 1A). Overall, 3T-iMRI contributed to upgrading of the resection level in 28 patients (34.1%).

### Residual tumor location

Further resection after iMRI was performed in 39 of the overall group of 82 patients. The locations of residual tumor eligible for further resection were cavernous sinus (21), suprasellar (15), intrasellar (11), and subdural (4; note that there was some overlap). Examples of residual tumor leading to further resection are presented in Figs. 1B–1E and

Figs. 2A–C. Figure 1B shows the multi-lobular recurrent adenoma compressing the optic chiasm. In Fig. 1C, after the descent of suprasellar arachnoid, the residual tumor was hidden by the fibrous septum (arrow) and iMRI revealed residual tumor in the cavernous sinus and subdural space under the septum (Fig. 1D), and additional removal of adenoma was performed (Fig. 1E). For these further resections, the image data in the neuronavigation system were upgraded and second-look surgery was performed. Of note, the 3T-iMRI detected a small residual tumor behind the internal carotid artery (ICA) that could be missed by endoscope and possibly by low-field MRI. A GHoma (Fig. 2A) appeared to be successfully removed following iMRI (Fig. 2B), but the axial image revealed a residual mass behind the ICA (arrow; Fig. 2C). The neuronavigation images were updated and the residual tumor was precisely located, with total removal being achieved. Postoperatively, the GH level and IGF-1 level of the patient were normalized.

### Detection of complications by iMRI

Two cases of intraoperative hematoma within the removal cavity were detected by iMRI. Both patients had a macroadenoma with suprasellar lobulation. Representative images are shown in Figs. 2D and 2E. Intraoperative hematoma evacuation was quickly performed without any morbidity.

### Postoperative complications

There was no intraoperative difficulty acquiring the 3T-iMRI data. Postoperative complications included CSF leak in one patient, permanent diabetes insipidus in three patients, new hypopituitarism in four patients, disturbance of visual function in one patient, hematoma at the abdominal fat graft harvest site in one patient, harvest site infection in one patient, and delayed nasal bleeding that required surgical hemostasis in one patient. There were no mortalities.

### Factors for predicting further resection following 3T-iMRI

To develop a new scoring system, patients were divided into a discovery cohort (56 patients) and a validation cohort (26 patients). The demographics of the two cohorts did not differ significantly (Table 1). Factors for predicting additional resection of the tumor following 3T-iMRI were selected by univariate analysis in the discovery cohort. The variables included were gender, age, preoperative maximum tumor diameter, Knosp grade, the number of past surgery, suprasellar lobulation ratio, and intention for complete resection. Among these variables, maximal tumor diameter ( $p = 0.046$ ), suprasellar

**Table 1** Patients' baseline characteristics

Characteristics	Overall (n = 82)	%	Discovery cohort (n = 56)	Validation cohort (n = 26)	<i>P</i>
Age, mean (SD) (years)	55.8 (13.9)		54.6 (14.6)	58.3 (12.0)	0.23
Female	51	62.2	37	14	0.29
Pathology					
Non-functioning	56	68.3	36	20	
GH-secreting	14	17.1	11	3	
Prolactin-secreting	5	6.1	5	0	
ACTH-secreting	4	4.9	1	3	
TSH-secreting	3	3.7	3	0	
Prior surgery					
0	57	69.5	41	16	0.421
1	18	22.0	10	8	
2 or above	7	8.5	5	2	
Knosp classification					
Grade 0	1	1.2	1	0	0.134
Grade 1	15	18.2	7	8	
Grade 2	23	28.0	16	7	
Grade 3	28	34.1	20	8	
Grade 4	15	18.3	12	3	
Lobulation ratio Mean (SD)	1.10 (0.20)		1.09 (0.19)	1.13 (0.23)	0.471
Max diameter Mean (SD) (mm)	23.8 (8.3)		23.6 (7.47)	24.2 (10.1)	
Intended GTR	63	76.8	41	22	0.286
Intended STR	19	23.2	15	4	

ACTH: adrenocorticotropic hormone, GH: growth hormone, TSH: thyroid-stimulating hormone.

lobulation ratio ( $p = 0.049$ ), and Knosp grade ( $p = 0.019$ ) exhibited significant associations with additional resection. The number of recurrences showed a trend for an association with additional resection ( $p = 0.051$ ).

Among these variables, Knosp grade showed a strong and significant association with maximal tumor diameter ( $r = 0.425$ ,  $p = 0.0011$ ; Supplementary Fig. 1A. All Supplementary Figs are available online.). Therefore, the maximal tumor diameter was selected as one of the variables. As discussed in more detail later, Knosp grade exhibited no significant influence on the risk of additional resection in the multiple-logistic regression analysis after adjustment for maximal tumor diameter.

Regarding the number of prior surgeries, there were seven patients with prior multiple surgical history, and six (83.3%) of them underwent additional tumor resection. The reasons for preventing maximal removal before iMRI for these seven patients were fibrous septum and scarring tissue due to the

prior operation, which could be detected only by iMRI. For these reasons, the history of past surgery was selected as one of the variables.

### ROC analysis

To determine the cutoff value for maximal diameter, ROC analysis was performed. For the maximal tumor diameter, a cutoff value 20 mm was chosen (Supplementary Fig. 2A) with sensitivity of 81% and a specificity of 55%. Suprasellar lobulation ratio was defined as the ratio between the maximal suprasellar horizontal diameter and the diaphragm, with the ratio defined as 1 when there was no suprasellar extension (Fig. 3A). Most of the patients had suprasellar lobulation ratio of 1.0 ( $n = 51$ ). For multi-lobular adenomas, the maximal suprasellar horizontal diameter was defined as the maximal distance between the farthest lobulation (Fig. 3B). A cutoff value 1.1 was chosen based on the ROC analysis (Supplementary Fig. 2B) with sensitivity of 40.7% and specificity of 96.6%.

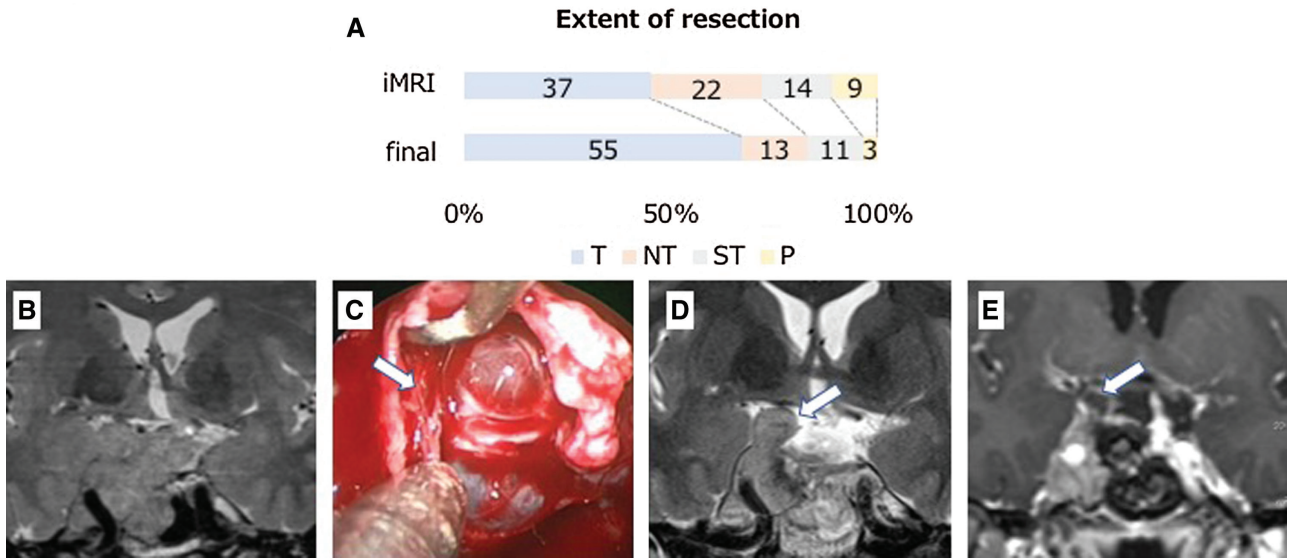


**Fig. 1** (A) The extent of pituitary adenoma resection following intraoperative MRI and final MRI (n = 82). T = total resection, 100%; NT = near total resection, 95% or greater; ST = subtotal resection, 80%–95%; P = partial resection of less than 80%. (B–E) Illustrative cases of iMRI images for multi-lobular recurrent adenoma. Recurrent non-functioning lobulated pituitary adenoma with planned subtotal resection (B) was removed by an endonasal endoscopic approach. After the initial resection, the descent of arachnoid was confirmed but the fibrous septum created by the previous operation was found on the right side (arrow) (C). 3T-iMRI showed residual tumor in the cavernous sinus and subdural space under the septum (arrow) (D) requiring second-look surgery. The second iMRI showed additional removal of the tumor (E). 3T-iMRI: 3-Tesla intraoperative high-field magnetic resonance imaging.

### Proposed pituitary score (Kyoto Pituitary Score)

Based on these findings, a new simple scoring system for pituitary adenoma surgery (Fig. 3C) was constructed. The new scoring system (range: 0–4) is a summation of three variables: the maximum diameter of the tumor (>20 mm: 1 point, ≤20 mm: 0 point), suprasellar tumor lobulation (suprasellar lobulation ratio >1.1: 1 point, ≤1.1: 0 point) and the presence of history of prior surgeries (1 point). The area under the ROC curve (AUROC) for the prediction of additional resection by 3T-iMRI was 0.732 ( $p = 0.0032$ ), which was higher than when these variables were included individually (AUROC 0.645 for maximal tumor diameter, 0.669 for suprasellar lobulation ratio, and 0.567 for the number of prior operation), confirming the improved accuracy of the model (Fig. 3D and Supplementary Figs. 2A and 2B). When applied to the discovery cohort, 13 patients were classified as a score of 0, 25 as a score of 1, 15 as a score of 2, and 4 as a score of 3. As shown in Fig. 3E, the proportion of patients who had additional resection after 3T-iMRI was 30.8% for a score of 0, 32.0% for a score of 1, 73.3% for a score of 2 and 100% for a score of 3, showing a significant linear trend ( $p = 0.0116$  for trend).

### Internal validation of the scoring system

The scoring system was internally validated by applying it to the validation cohort (n = 26). The

system classified the 26 patients in the validation cohort, with two patients classified as 0 points, 13 as 1 point, 10 as 2 points, and 1 as 3 points. As shown in Fig. 3E, additional resection after 3T-iMRI was performed in 0% of patients with score 0, 30.8% with score 1, 70.0% with score 2, and 100% with score 3 ( $p = 0.0037$  for trend). Overall, the proposed scoring system was able to effectively discriminate between patients who were likely to undergo further resection using 3T-iMRI.

### Multiple logistic regression analysis

Factors for predicting additional resection of the tumor following 3T-iMRI were assessed by building multiple logistic regression models for overall patients. The variables included age, sex, preoperative maximum tumor diameter, Knosp grade, the number of prior surgeries, suprasellar lobulation ratio, and intended subtotal resection. A stepwise regression model showed that the maximal tumor diameter ( $p = 0.012$ ), the number of prior surgeries ( $p = 0.056$ ), and the suprasellar lobulation ratio ( $p = 0.088$ ) were significantly associated with higher chances of having additional resection after the iMRI examination (Table 2; model 1). Because Knosp grade was significantly associated with the chance of undergoing additional resection after iMRI according to a comparison using Student's *t*-test in

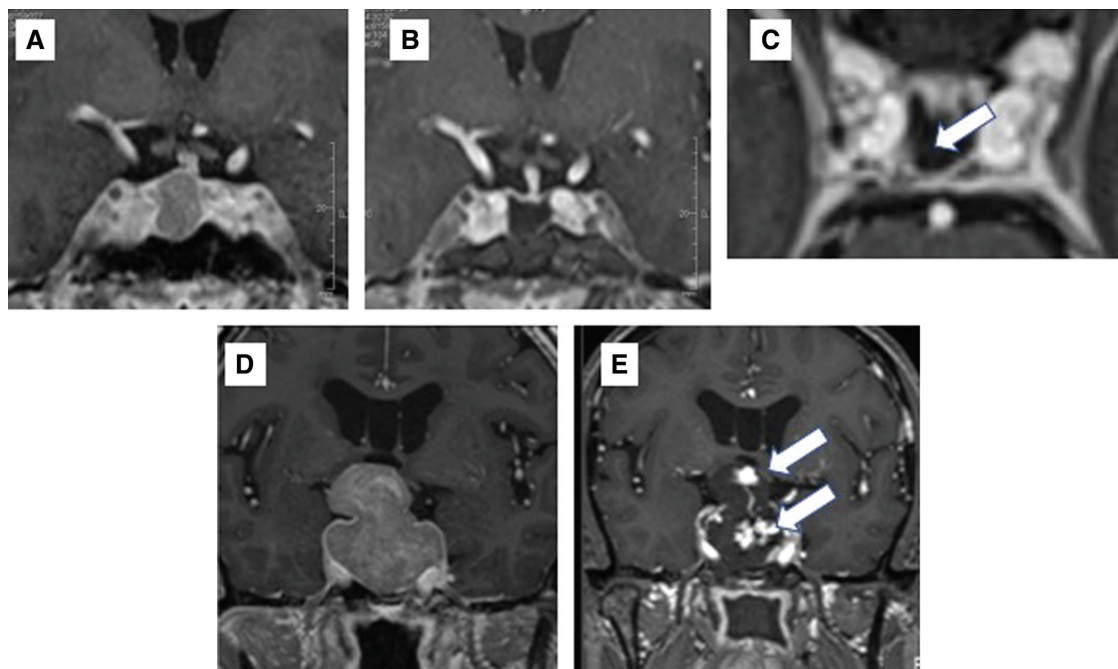


**Fig. 2 (A–C)** Illustrative cases of iMRI images for small residual tumor. A GHoma (A) appeared to be successfully removed following iMRI (B), but the axial image revealed a residual mass behind the ICA (arrow) (C). The neuronavigation images were updated and the residual tumor was precisely located, with total removal achieved. **(D–E)** Illustrative cases of early hematoma detection. Preoperative MRI of a lobulated tumor is shown in (D). Intraoperative MRI showed contrast agent extravasation in the removal cavity, indicating hematoma formation (E). ICA: internal carotid artery.

the discovery cohort, we intentionally added this covariate into the model (Table 2; model 2). The addition of Knosp grade did not influence the results of the regression analysis ( $p = 0.864$ ). We then tested whether Knosp grade was confounded by any of the variables and found that the maximum tumor diameter showed a significant linear correlation with Knosp grade (Supplementary Fig. 1A). Incorporation of Knosp grade into the Kyoto Pituitary Score did not improve the prediction accuracy, as shown in Supplementary Fig. 1B.

## Discussion

### High-field intraoperative MRI for pituitary adenoma resection

iMRI has been increasingly used in pituitary surgery since its introduction in 1994.<sup>15</sup> A previous literature review including 24 studies<sup>10</sup> found an average initial GTR rate of 51% and a final GTR rate of 73%. Conversely, a recent meta-analysis found GTR rates of 79% and 65% for pure endoscopic and pure microsurgical series, respectively. The current study suggested that surgeons who had iMRI available tended to be less aggressive in the initial resection before iMRI compared with surgeons who did not

have iMRI available.<sup>9</sup> We may be biased toward a less aggressive approach before iMRI. Upgrading of the resection level was achieved in 34.1% of the overall patient cohort, which confirmed that 3T-iMRI could help to increase the tumor resection rate beyond the capabilities of endoscopic surgery alone.

The number of reports using high-field intraoperative MRI for pituitary adenoma has increased in recent years.<sup>3</sup> High-field systems require a substantial investment, as the construction of the operating theatre and shielding must be appropriate. However, compared with low-field systems, these systems provide higher-resolution images with a shorter acquisition time.<sup>16</sup> A recent clinical trial<sup>17</sup> investigating the performance of high-field iMRI in transphenoidal surgery failed to demonstrate the superiority of iMRI, but concluded that, for less experienced surgeons, this method helped to optimize the resection rate without causing an increase in complications. However, this clinical trial mixed experienced surgeons with a tendency to use an endoscope with less experienced surgeons who tended to favor a microsurgical approach. Thus, it is difficult to interpret the data.

Previous reports of the combination of endoscopy with high-field MRI are limited. The first report<sup>6</sup>

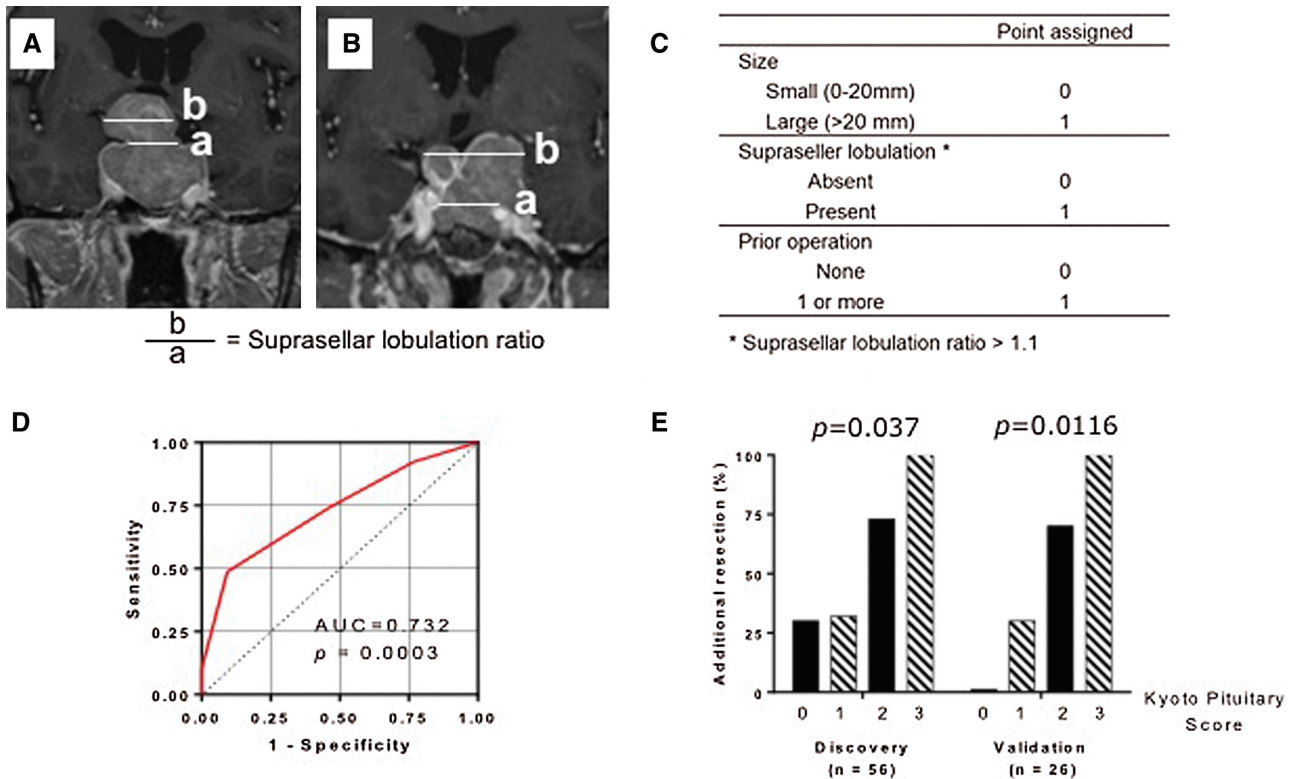


**Fig. 3** (A) Measurement of suprasellar lobulation. Suprasellar lobulation ratio was defined as a ratio between the maximal suprasellar horizontal diameter and the diaphragm. The maximal horizontal diameter of the tumor in the suprasellar area was measured with coronal preoperative contrast-enhanced T1-weighted imaging (b). The diameter of the diaphragm defect was also measured on coronal slices. When it was not apparent, the measurement was performed at the level of the most proximal C2 portion of the carotid on contrast-enhanced T1-weighted images (a). When there was no suprasellar extension, the ratio was defined as 1. (B) Measurement of multi-lobular adenoma. For multi-lobular tumor, the maximal suprasellar horizontal diameter was defined as the maximal distance between the farthest lobulation. (C) Kyoto Pituitary Score. The new scoring system (range: 0–4) is the summation of three variables: the maximum diameter of the tumor (>20 mm: 1 point, ≤20 mm: 0 points), suprasellar tumor lobulation (suprasellar lobulation ratio >1.1: 1 point, ≤1.1: 0 points) and the presence of history of prior surgeries (1 point). (D) ROC analysis for the Kyoto Pituitary Score. The AUROC was 0.732 ( $p = 0.0003$ ). (E) Rates of additional resection following 3T-iMRI stratified by the Kyoto Pituitary score in the discovery cohort (0 points, 30.8%; 1 point, 32.0%; 2 points, 73.3%; 3 points, 100%;  $p = 0.0037$  for trend) and validation cohort (0 points, 0%; 1 point, 30.8%; 2 points, 70.0%; 3 points, 100%;  $p = 0.0116$  for trend). AUROC: area under the ROC curve, ROC: receiver operating characteristic, 3T-iMRI: 3-Tesla intraoperative high-field magnetic resonance imaging.

on this subject included 86 adenoma patients and demonstrated that, in the group of patients for which GTR was planned, iMRI led to additional resection in 22.4% of cases, while in the group for whom subtotal resection was planned, additional resection was performed in 48.7% of cases. The use of iMRI increased the GTR rate from 69.6% to 91.8% overall. A second report<sup>5)</sup> including 20 macroadenoma patients showed that unexpected residual tumor was found on iMRI in 30% of patients, and that iMRI helped extend the GTR rate from 60% to 80%. The current results are in accord with these previous findings and support the conclusion<sup>18)</sup> that although endoscopes provide highly magnified, clear views,

the surgeon's interpretation of intraoperative findings may be challenging because of the similarity between hyperemic normal gland and residual tumor. Intraoperative image guidance has the power to correct the surgeon's misinterpretation and provide the surgeon with instant feedback before the end of surgery. This may increase the safety of surgery and extend the extent of surgery.

Image artifacts due to blood from the tumor and the detection of devascularized tumor remain challenging.<sup>19)</sup> We mostly assessed post-contrast T1-weighted images, but when necessary, we compared preoperative and intraoperative images, not only post-contrast T1-weighted images but also T2 or FLAIR sequences.

**Table 2 Univariate and multivariate logistic regression analyses of risk factors associated with additional resection after iMRI in endonasal surgery for pituitary adenoma**

Variables	Model 1		Model 2	
	Odds ratio (95% CI)	<i>p</i>	Odds ratio (95% CI)	<i>p</i>
Maximum tumor diameter	1.11 (1.04–1.19)	0.012	1.10 (1.01–1.08)	0.017
Suprasellar lobulation ratio	25.6 (0.61–1068.1)	0.089	24.3 (0.56–1051.8)	0.097
Number of prior surgeries	2.31 (0.98–5.44)	0.056	2.28 (0.95–5.43)	0.064
Knosp classification	NA	NA	1.05 (0.62–1.77)	0.864

Model 1 was obtained using a stepwise method. Model 2 was calculated by adding Knosp grade as a covariate. iMRI: intraoperative high-field magnetic resonance imaging.

Comparison of these images helped to differentiate image artifacts from tumor remnants. Further research is needed to develop methods for overcoming image artifacts, and pathological investigation of the removed remnants is likely to be helpful.

#### **Newly proposed scoring system (Kyoto Pituitary Score) to predict the benefits of intraoperative MRI**

The new scoring system proposed in this study is simple, being based on three variables: the maximum diameter of the tumor, the presence of suprasellar lobulation (the ratio between the maximal suprasellar diameter and the diaphragm), and the number of prior transsphenoidal surgeries. This scoring system exhibited robust interclass differences in predicting the need for iMRI for further resection of the tumor both in the discovery and in the validation cohort. The proposed score could also be considered for prediction of unintentional tumor remnants, even with the use of an endoscope and neuronavigation, and could potentially influence surgical strategy before termination of the procedure at institutions without iMRI.

Several factors influencing the likelihood of GTR have been previously reported.<sup>20–22</sup> The best known classification is the Knosp grade, which is based on the qualitative assessment of tumor morphology<sup>21,22</sup> and has been widely adopted because of its relatively simple definition. However, some authors have pointed out the relatively weak inter-observer agreement of this approach, and suggested pooling the lower Knosp grades (0,1,2) into one grade should be performed to improve inter-rater reliability.<sup>23</sup> The Knosp grade is highly effective for assessing the likelihood of cavernous sinus invasion of the tumor. However, in the current study, the Knosp grade itself was not a strong predictor of the detection of unexpected residual tumor requiring further resection when a multiple regression model for the whole cohort was constructed, possibly because cavernous sinus invasion (as in Knosp 4 tumors) remained

untouched, even after detection by iMRI, or because of the confounding influence of tumor diameter. Currently, high-field MRI is only available at a limited number of centers, and little is known about the specific utility of 3T-iMRI in different subsets of patients with pituitary adenoma. The Zurich pituitary score was devised to address this problem<sup>12</sup> using a four-tier score based on quantitative measurement of the tumor,<sup>11</sup> the maximum horizontal diameter of the adenoma, and the minimal distance at the intracavernous horizontal C4 segment of the ICA. It has been reported that the Zurich pituitary score can predict the utility of iMRI in transsphenoidal pituitary adenoma surgery<sup>12</sup>; however, the study reporting this result also found that the clinical utility of 3T-iMRI was greatest for simple cases (classes I–II) rather than complex cases (classes III–IV), contrary to the current findings. The reasons for their paradoxical finding regarding the utility of iMRI may be explained by a low rate of conversion to total resection in complex cases that cannot be resected, even when iMRI is performed. However, the benefit of iMRI for complex tumors must include the imaging of specific parts of tumors that could compress the optic chiasm,<sup>5</sup> the early detection of hematoma formation, and cases subject to surgical disorientation, as in multi-lobular tumors. The currently proposed scoring system is unique in incorporating the effect of prior transsphenoidal surgery in the prediction of difficulty obtaining satisfactory resection without iMRI. The presence or absence of prior surgery was found to be a predictor of the detection of tumor remnants suitable for further resection, as shown in Figs. 1B–1E. This is mostly due to the scar tissue within the tumor and intratumoral septum, which prevents surgical resection, even with the use of an endoscope and neuronavigation. We also consider that the utility of iMRI lies not only in GTR of the tumor but also in the detection of unexpected residual tumor leading to further resection. In our scoring system, iMRI



was more beneficial for complex cases, such as those with large lobulated tumors and prior surgical history.

### Limitations

Final judgments regarding the overall impact of intraoperative MRI should be based on long-term recurrence rates. The current study was performed within a relatively short period of time, and it may take years for recurrence to be fully elucidated because most pituitary adenomas are benign and slow growing. Furthermore, as the current study was a retrospective analysis, a patient selection bias is possible, even though we routinely use iMRI for pituitary adenoma surgery for scheduled cases. Finally, all data in the current study were from the same surgical team and could potentially be affected by technical and institutional bias. Thus, further external validation of the scoring system, ideally using a prospective study design, is needed to elucidate the effectiveness of the method.

### Conclusion

3T-iMRI satisfactorily depicted unexpected residual tumor and optimized the extent of tumor resection. Our newly proposed scoring system (Kyoto Pituitary Score) predicted the usefulness of iMRI for each patient and stratified the possibility of unintentional residual tumor, even with an endoscope guided by a navigation system. We propose that patients with large lobulated adenomas with prior surgical history benefit most from the use of iMRI.

### Acknowledgments

We thank Karl Embleton, PhD and Benjamin Knight, MSc., from Edanz Group ([www.edanzediting.com/ac](http://www.edanzediting.com/ac)) for editing a draft of this manuscript.

### Conflicts of Interest Disclosure

All authors declare that they have no conflict of interest.

### References

- 1) Kassam AB, Prevedello DM, Carrau RL, et al.: Endoscopic endonasal skull base surgery: analysis of complications in the authors' initial 800 patients. *J Neurosurgery* 114: 1544–1568, 2011
- 2) de Divitiis E, Laws ER, Giani U, Iuliano SL, de Divitiis O, Apuzzo ML: The current status of endoscopy in transsphenoidal surgery: an international survey. *World Neurosurg* 83: 447–454, 2015
- 3) Soneru CP, Riley CA, Hoffman K, Tabaei A, Schwartz TH: Intra-operative MRI vs endoscopy in achieving gross total resection of pituitary adenomas: a systematic review. *Acta Neurochir (Wien)* 161: 1683–1698, 2019
- 4) Fahlbusch R, Golby A, Prada F, Zada G: Utility of intraoperative imaging. *Neurosurg Focus* 40: 1610, 2016
- 5) Zaidi HA, De Los Reyes K, Barkhoudarian G, et al.: The utility of high-resolution intraoperative MRI in endoscopic transsphenoidal surgery for pituitary macroadenomas: early experience in the advanced multimodality image guided operating suite. *Neurosurg Focus* 40: E18, 2016
- 6) Netuka D, Masopust V, Belšán T, Kramář F, Beneš V: One year experience with 3.0 T intraoperative MRI in pituitary surgery. *Acta Neurochir Suppl* 109: 157–159, 2011
- 7) García S, Reyes L, Roldán P, et al.: Does low-field intraoperative magnetic resonance improve the results of endoscopic pituitary surgery? Experience of the implementation of a new device in a referral center. *World Neurosurg* 102: 102–110, 2017
- 8) Pal'a A, Knoll A, Brand C, et al.: The value of intraoperative magnetic resonance imaging in endoscopic and microsurgical transsphenoidal pituitary adenoma resection. *World Neurosurg* 102: 144–150, 2017
- 9) Schwartz TH, Stieg PE, Anand VK: Endoscopic transsphenoidal pituitary surgery with intraoperative magnetic resonance imaging. *Neurosurgery* 58: 44–51, 2006
- 10) Serra C, Burkhardt JK, Esposito G, et al.: Pituitary surgery and volumetric assessment of extent of resection: a paradigm shift in the use of intraoperative magnetic resonance imaging. *Neurosurg Focus* 40: E17, 2016
- 11) Serra C, Staartjes VE, Maldaner N, et al.: Predicting extent of resection in transsphenoidal surgery for pituitary adenoma. *Acta Neurochir (Wien)* 160: 2255–2262, 2018
- 12) Staartjes VE, Serra C, Maldaner N, et al.: The Zurich Pituitary Score predicts utility of intraoperative high-field magnetic resonance imaging in transsphenoidal pituitary adenoma surgery. *Acta Neurochir (Wien)* 161: 2107–2115, 2019
- 13) Sylvester PT, Evans JA, Zipfel GJ, et al.: Combined high-field intraoperative magnetic resonance imaging and endoscopy increase extent of resection and progression-free survival for pituitary adenomas. *Pituitary* 18: 72–85, 2015
- 14) Esposito F, Dusick JR, Fatemi N, Kelly DF: Graded repair of cranial base defects and cerebrospinal fluid leaks in transsphenoidal surgery. *Oper Neurosurg (Hagerstown)* 60: 295–303; discussion 303–304, 2007
- 15) Black P, Jolesz FA, Medani K: From vision to reality: the origins of intraoperative MR imaging. *Acta Neurochir Suppl* 109: 3–7, 2011
- 16) Pinker K, Ba-Ssalamah A, Wolfsberger S, Mlynarik V, Knosp E, Trattning S: The value of high-field MRI (3T) in the assessment of sellar lesions. *Eur J Radiol* 54: 327–334, 2005
- 17) Tandon V, Raheja A, Suri A, et al.: Randomized trial for superiority of high field strength intraoperative magnetic resonance imaging guided

- resection in pituitary surgery. *J Clin Neurosci* 37: 96–103, 2017
- 18) Jane JA, Laws ER: Endoscopy versus MR imaging. *J Neurosurg* 112: 734, discussion 735, 2010
- 19) Buchfelder M, Schlaffer SM: Intraoperative magnetic resonance imaging during surgery for pituitary adenomas: pros and cons. *Endocrine* 42: 483–495, 2012
- 20) Hardy J, Vezina JL: Transsphenoidal neurosurgery of intracranial neoplasm. *Adv Neurol* 15: 261–273, 1976
- 21) Knosp E, Steiner E, Kitz K, Matula C: Pituitary adenomas with invasion of the cavernous sinus space: a magnetic resonance imaging classification compared with surgical findings. *Neurosurgery* 33: 610–617; discussion 617–618, 1993
- 22) Micko AS, Wöhrer A, Wolfsberger S, Knosp E: Invasion of the cavernous sinus space in pituitary adenomas: endoscopic verification and its correlation with an MRI-based classification. *J Neurosurg* 122: 803–811, 2015
- 23) Mooney MA, Hardesty DA, Sheehy JP, et al.: Interrater and intrarater reliability of the Knosp scale for pituitary adenoma grading. *J Neurosurg* 126: 1714–1719, 2017

---

Corresponding author: Masahiro Tanji, MD  
Department of Neurosurgery, Kyoto University Graduate School of Medicine, 54 Shogoinkawaharacho, Sakyo-ku, Kyoto, Kyoto 606-8507, Japan.  
*e-mail:* tanji@kuhp.kyoto-u.ac.jp